

Synthesis and Characterization of a Liquid Crystal-Modified Polydimethylsiloxane Rubber with Mechanical Adaptability Based on Chain Extension in the Process of Crosslinking

Zhe Liu, Hua Wang,* and Chuanjian Zhou*

Cite This: *ACS Omega* 2022, 7, 36590–36597

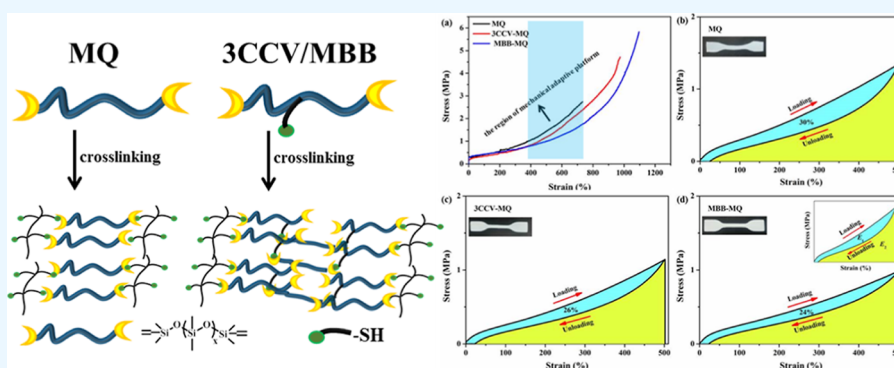
Read Online

ACCESS |

Metrics & More

Article Recommendations

Supporting Information



ABSTRACT: The mechanical adaptive material is a kind of functional material that can effectively dissipate energy and suppress the increase of its stress under continuous strain in a large deformation area, which are vital in artificial muscles, connection devices, soft artificial intelligence robots, and other areas. Scientists have been working to broaden the platform of the material's mechanical adaptive platform and improve its mechanical strength by specific structure design. Based on it, we expect to introduce a mechanism of energy dissipation from the molecular chain scale to further improve mechanical adaptability. We developed a liquid crystal-modified polydimethylsiloxane rubber with mechanical adaptability based on chain extension in the process of crosslinking. Results showed that liquid crystal (0.7 mol %)-modified silicone rubber can obviously dissipate energy to achieve mechanical adaptive function, and the energy dissipation ratio of polydimethylsiloxane rubber (MQ), 4-propyl-4'-vinyl-1,1'-bi(cyclohexane)-modified polydimethylsiloxane rubber (3CCV-MQ), and 4-methoxyphenyl-4-(3-butenyloxy) benzoate-modified polydimethylsiloxane rubber (MBB-MQ) gradually decreases from 30 to 24%. Excessive thiol groups of liquid crystal-modified polydimethylsiloxane react with its vinyl group to achieve the chain extension, which significantly improves the mechanical strength from 2.74 to 5.83 MPa and elongation at break from 733 to 1096%. This research offers some new insights into improving the mechanical strength of silicone rubber and is of great significance for the application of the mechanical adaptive material.

INTRODUCTION

The mechanical adaptive material is a key material in connection devices, artificial muscles, and other areas, which can effectively dissipate energy and suppress the increase of stress under continuous strain in a large deformation area.^{1–6} Several attempts have been made to broaden the platform of the material's mechanical adaptability and improve its mechanical strength.^{7,8} We expect to introduce a novel energy dissipation mechanism from the molecular chain scale to further improve mechanical adaptability. Among them, liquid crystal elastomers have become the forefront of recent research due to their characteristic energy dissipation mechanism, which can undergo internal phase transition under external stimulation.^{9–14} Recently, Yu et al. developed 3D-printing liquid crystal elastomer foams to enhance energy dissipation under mechanical insult.¹⁵ Frick's group investigated the

mechanical energy dissipation behavior in polydomain nematic liquid crystal elastomers in response to oscillating loading.¹⁶

Although many research groups have done a lot of work on liquid crystal elastomers,^{17–23} there is very little published research on its mechanical adaptability, and the mechanical tensile strength in previous literature almost never exceeds 1 MPa.^{24–28} Due to high- and low-temperature resistance, aging resistance, weather resistance, and other excellent characteristics,^{29–31} our group has been committed to developing

Received: July 19, 2022

Accepted: September 16, 2022

Published: October 3, 2022



Scheme 1. Detailed Synthesis Processes of (a) 3CCV/MBB-Modified Polydimethylsiloxane and (b) 3CCV/MBB-MQ

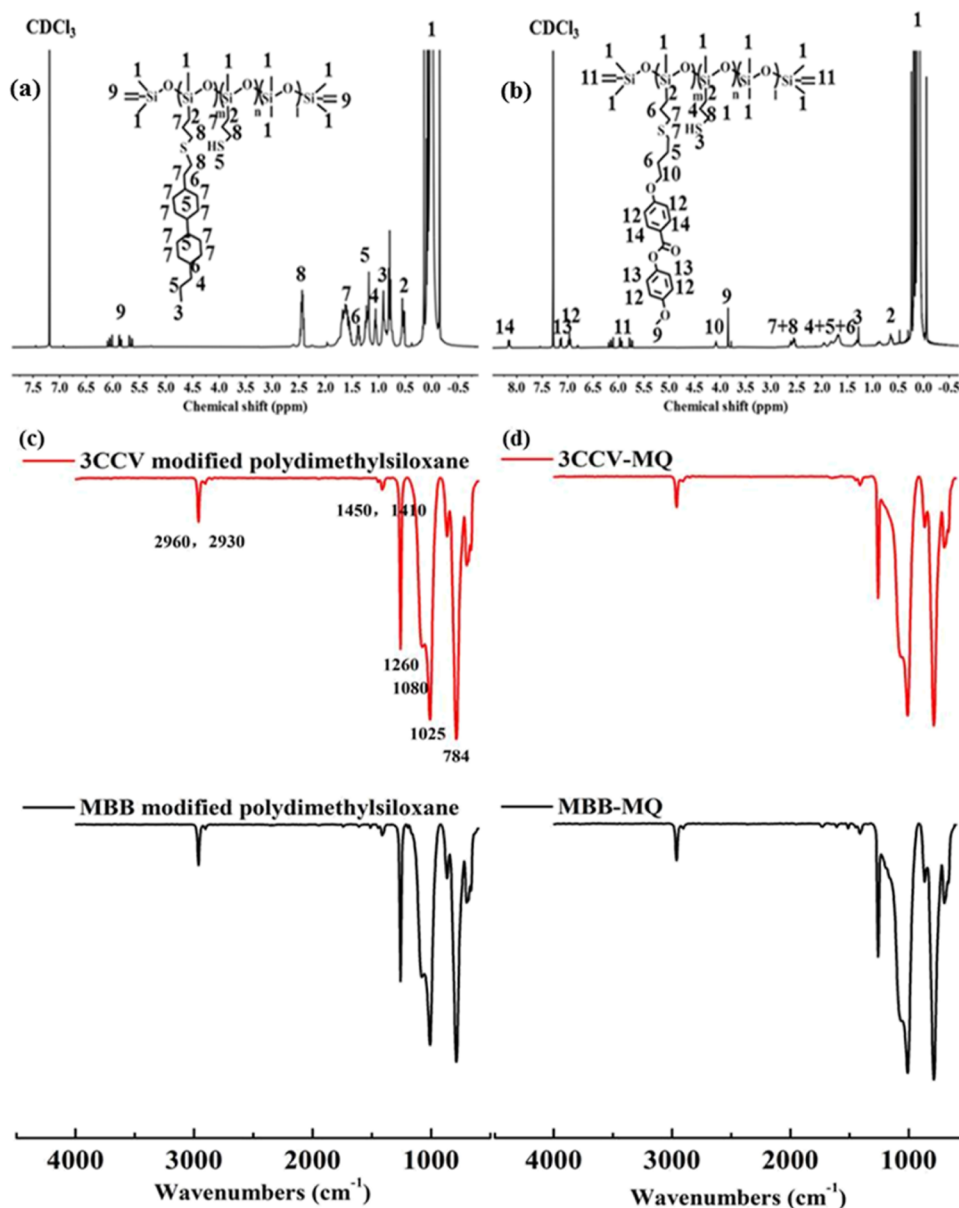
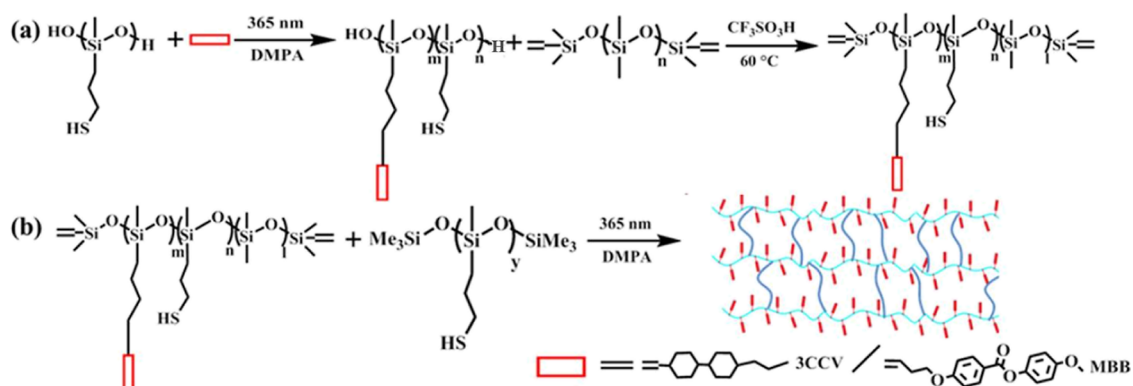


Figure 1. ^1H NMR spectra of (a) 3CCV-modified polydimethylsiloxane and (b) MBB-modified polydimethylsiloxane in CDCl_3 . FT-IR spectra of (c) 3CCV-modified polydimethylsiloxane and MBB-modified polydimethylsiloxane and (d) 3CCV-MQ and MBB-MQ.

mechanical adaptive materials based on polydimethylsiloxane to ensure the application of this material under harsh

environments, and commercially available PDMS-based elastomers do not perform this function. In our previous

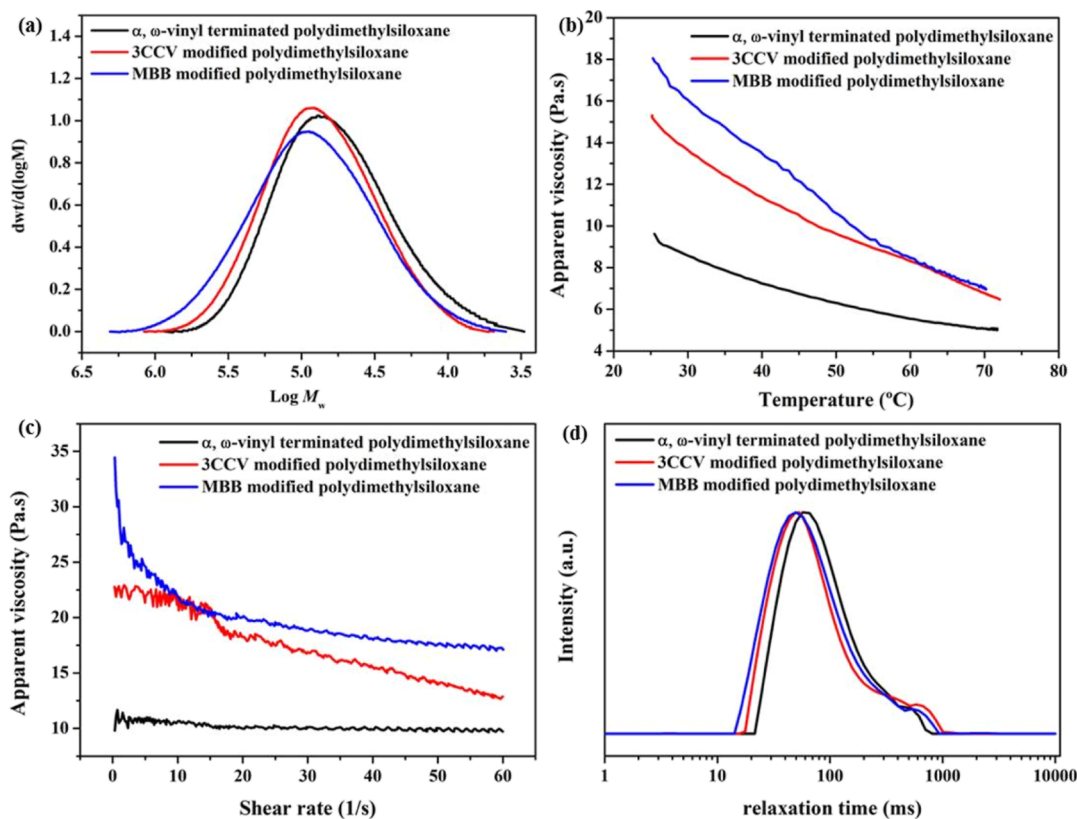


Figure 2. (a) GPC curves of α,ω -vinyl-terminated polydimethylsiloxane and 3CCV/MBB-modified polydimethylsiloxane using THF as an eluent. Viscosity curves of α,ω -vinyl-terminated polydimethylsiloxane and 3CCV/MBB-modified polydimethylsiloxane (b) at a shear rate of 40 s^{-1} against temperature and (c) at $25\text{ }^{\circ}\text{C}$ against shear rate. (d) Relaxation time of α,ω -vinyl-terminated polydimethylsiloxane and 3CCV/MBB-modified polydimethylsiloxane at $25\text{ }^{\circ}\text{C}$.

work, we developed several kinds of liquid crystal-based organosilicone elastomers with mechanical adaptability, whose mechanical tensile strength was up to 4 Mpa.^{32,33} However, the production process of introducing the crosslinking system with liquid crystal units as the crosslinking center in our previous study is complicated, and it is very difficult to prepare large size samples for practical applications.^{34–37}

Hence, we developed a liquid crystal-modified polydimethylsiloxane rubber with mechanical adaptability based on chain extension in the process of crosslinking by ingenious structure design. This strategy not only realizes mechanical adaptability from the molecular chain scale but also greatly improves the mechanical strength of silicone rubber. The structure of 3CCV/MBB-modified polydimethylsiloxane was synthesized and characterized by nuclear magnetic resonance hydrogen spectrum (^1H NMR), Fourier transform infrared spectroscopy (FT-IR), and gel permeation chromatography (GPC). Apparent viscosity and relaxation time were performed to study the rheological behavior of 3CCV/MBB-modified polydimethylsiloxane. The stress–strain test indicates that 3CCV/MBB-MQ can dissipate energy to achieve mechanical adaptive function and the mechanical adaptive platform of 3CCV-MQ is not as obvious as MBB-MQ, but it is clearer than MQ. Excessive thiol groups of 3CCV/MBB-modified polydimethylsiloxane react with its vinyl group to achieve the effect of chain extension, which significantly improves the mechanical strength and elongation at break of 3CCV/MBB-MQ compared with MQ.^{38,39} It provides fresh insight into ways to further improve the mechanical properties of silicone rubber. Our findings make an important contribution to the

development of elastomers with mechanical adaptability, which is of great significance for the application of this key material.

RESULTS AND DISCUSSION

The synthesis of 3CCV/MBB-modified polydimethylsiloxane is divided into two steps: (1) synthesis of the 3CCV/MBB-modified mercaptopropyl silicone oil prepolymer and (2) ring–opening equilibrium polymerization of the 3CCV/MBB-modified mercaptopropyl silicone oil prepolymer and α,ω -vinyl-terminated polydimethylsiloxane. In our early exploration, the incompatibility between 3CCV/MBB and polydimethylsiloxane leads to a serious problem of an incomplete ring–opening equilibrium polymerization. Herein, We synthesized 3CCV/MBB (0.7 mol %)-modified-terminated polydimethylsiloxane by grafting 3CCV/MBB to hydroxyl-terminated mercaptopropyl silicone oil prepolymer and then reacting with α,ω -vinyl-terminated polydimethylsiloxane with the help of solvent. The detailed synthesis processes are shown in Scheme 1. The composition of 3CCV/MBB-modified polydimethylsiloxane is listed in Table S1.

As shown in Figure 1a,b, all the chemical shifts of ^1H NMR spectra correspond to the structure of the polymer, indicating that we successfully prepared 3CCV/MBB-modified polydimethylsiloxane. In order to obtain complete grafting of 3CCV/MBB, we fed an excess of thiol groups. ^1H NMR spectra also do not show the vinyl peak of 3CCV/MBB, which further indicates the grafting efficiency of 3CCV/MBB is 100%. Due to the low molar ratio of 3CCV/MBB-modified polydimethylsiloxane, the integral area is of little significance.

Table 1. Summary of M_n , M_w , M_v , and PDI of α,ω -Vinyl-Terminated Polydimethylsiloxane and 3CCV/MBB-Modified Polydimethylsiloxane

no.	M_n /(g/mol)	M_w /(g/mol)	M_v /(g/mol)	PDI
α,ω -vinyl-terminated polydimethylsiloxane	38,700 ^a	84,000 ^a	51,200 ^b	2.17
3CCV-modified polydimethylsiloxane	51,900 ^a	104,000 ^a	63,750 ^b	2
MBB-modified polydimethylsiloxane	52,400 ^a	131,000 ^a	65,520 ^b	2.5

^aDetermined by GPC. ^bDetermined by an Ubbelohde viscometer.

In the FTIR-ATR spectra of 3CCV/MBB-modified polydimethylsiloxane, the absorption peak near 1260 cm^{-1} is the symmetrical deformation vibration absorption peak of CH_3 on Si–Me and the absorption peak near 784 cm^{-1} is the plane rocking vibration of CH_3 and the stretching vibration absorption peak of Si–C, respectively. The strong and wide absorption peaks near 1080 and 1025 cm^{-1} are the stretching vibration absorption peak of Si–O–Si. The absorption peaks near 1460 and 1410 cm^{-1} are the antisymmetric deformation vibration absorption peak of CH_3 and the shear vibration absorption peak of CH_2 . The strong absorption peak near 2960 and 2930 cm^{-1} is the C–H stretching vibration absorption peak of CH_3 and CH_2 (Figure 1c,d). All absorption peaks in the FTIR-ATR spectrum can correspond to the structure of silicone oil. Because of the low molar ratio of 3CCV/MBB of 3CCV/MBB-modified polydimethylsiloxane, the characteristic peak of 3CCV/MBB in the infrared spectrum is not obvious.

3CCV/MBB-MQ was prepared by thiol–ene click reaction of 3CCV/MBB-modified polydimethylsiloxane and polymethylmercaptopropylsiloxane. The nano-silica (H2000) is used as a reinforcing filler to improve the mechanical strength of silicone rubber. Two different liquid crystal-modified silicone rubber (3CCV-MQ and MBB-MQ) were prepared and compared with MQ. Excessive thiol groups were used to make sure that 3CCV/MBB is completely connected to hydroxyl-terminated mercaptopropyl silicone oil prepolymer. Therefore, in order to ensure that the crosslinking density of the elastomers is basically the same, the amount of polymethylmercaptopropylsiloxane for MQ should be reduced as appropriate. The specific details are summarized in Table S2.

We carried out GPC characterization to further study the properties of 3CCV/MBB-modified polydimethylsiloxane. Figure 2a shows that the GPC curve of 3CCV/MBB-modified polydimethylsiloxane displays unimodal, demonstrating excellent equilibrium polymerization process. As shown in Table 1, the number average molecular weight (M_n), weight average molecular weight (M_w), and viscosity average molecular weight (M_v) of 3CCV/MBB-modified polydimethylsiloxane are larger than α,ω -vinyl-terminated polydimethylsiloxane, and the PDI value of all silicone oils are around 2. Moreover, the M_w and M_v of MBB-modified polydimethylsiloxane are larger than that of 3CCV-modified polydimethylsiloxane. The reason is that the molar ratio of 3CCV/MBB is completely consistent, but the molecular weight of MBB is larger than 3CCV. The GPC curves indicate that 3CCV/MBB-modified polydimethylsiloxane has been successfully prepared and the molecular weight distribution is uniform. The PDI value is determined by the method of equilibrium polymerization.

In order to further explore the rheological properties of 3CCV/MBB-modified polydimethylsiloxane prepared by us, we measured the apparent viscosity of 3CCV/MBB-modified polydimethylsiloxane at different temperatures and shear rates. As shown in Figure 2b, the apparent viscosity of MBB-

modified polydimethylsiloxane is highest at room temperature, followed by 3CCV-modified polydimethylsiloxane and α,ω -vinyl-terminated polydimethylsiloxane. This can be attributed to the difference in the intermolecular force of the liquid crystal-modified polydimethylsiloxane. Although the molar ratio of 3CCV/MBB is low, there are still interactions between 3CCV/MBB-modified polydimethylsiloxane, resulting in the higher apparent viscosity of the system. In addition, the apparent viscosity of MBB-modified polydimethylsiloxane is higher than that of 3CCV-modified polydimethylsiloxane, which indicates that the intermolecular force between MBB with a large benzene ring structure is greater than that in 3CCV. When the temperature is higher than 60 $^\circ\text{C}$, the intermolecular force between 3CCV/MBB-modified polydimethylsiloxane is destroyed. The structure of the 3CCV and MBB-polydimethylsiloxane is basically the same, so the apparent viscosity of 3CCV and MBB-modified polydimethylsiloxane tends to be consistent. The apparent viscosity of all samples decreases with increasing temperature. With the increase in temperature, the activity of the polymer chain segment increases, the intermolecular force is weakened, and the fluidity of the polymer is enhanced. The intermolecular force between 3CCV/MBB-modified polydimethylsiloxane is also illustrated by the curve of viscosity with shear rate (Figure 2c). The apparent viscosity of all samples decreased with increasing shear rate, exhibiting the shear thinning behavior of a non-Newtonian fluid. As the shear rate increases, the polymer segment orientation overcomes not only the entanglement between the segments but also the intermolecular force between 3CCV/MBB-modified polydimethylsiloxane. Therefore, the viscosity of 3CCV/MBB-modified polydimethylsiloxane with shear rate shows a completely different trend compared with α,ω -vinyl-terminated polydimethylsiloxane. The difference in viscosity with temperature and shear rate is determined by the difference in the structure of the modified polydimethylsiloxane.

The relaxation time experiment was performed to further explore the structure of the polymer chain and its dynamics. The relaxation time curves of all samples showed only two peaks. Compared with α,ω -vinyl-terminated polydimethylsiloxane, the relaxation time of 3CCV/MBB-modified polydimethylsiloxane is shorter. The relaxation time of MBB-modified polydimethylsiloxane is shorter than 3CCV-modified polydimethylsiloxane, which further proves that the intermolecular force of MBB-modified polydimethylsiloxane is greater than that of 3CCV. The worse the motion of the polymer chain, the shorter the relaxation time (Figure 2d).

The proportion of crosslinking chains, dangling chains, free chains, and crosslinking density in MQ, 3CCV-MQ and MBB-MQ are shown in Table S3. The proportion of crosslinking chains in MQ is significantly lower than that in 3CCV-MQ and MBB-MQ because 3CCV/MBB-modified polydimethylsiloxane has a residual thiol group, which leads to the increase of crosslinking points of elastomers. The proportion of dangling

chains and free chains in MQ is significantly higher than in 3CCV-MQ and MBB-MQ. The explanation is that the differences in intermolecular force between 3CCV/MBB-modified polydimethylsiloxane lead to different spatial structures of 3CCV/MBB-MQ. MQ has fewer thiol group active sites than 3CCV-MQ and MBB-MQ, so there are more free chains after crosslinking. The crosslinking density of all the elastomers we prepared was around 0.95. By ensuring that the crosslinking density of the elastomers is basically the same, we eliminate the interference of crosslinking density on the mechanical properties of the elastomers and study the influence of liquid crystal types on the mechanical properties of the elastomers.

The thermal properties of 3CCV- and MBB-modified polydimethylsiloxane, 3CCV-MQ, and MBB-MQ were investigated by DSC. Previous research has shown the glass transition temperature (T_g) of dimethylsilicone rubber is about -123 °C, and it can crystallize near -100 °C.^{40,41} From Figure 3a, the T_g of 3CCV-MQ and MBB-MQ has no change compared with MQ, but the crystallization temperature of 3CCV- and MBB-modified MQ is higher than that of MQ. It can be attributed to the fact that the intermolecular force of 3CCV/MBB affects the crystallization of pure polydimethylsiloxane, so the crystallization temperature of 3CCV/MBB-MQ is higher than that of MQ. Interestingly, MBB-MQ starts crystallization at -75 °C and 3CCV-MQ starts crystallization at -80 °C. As the interaction force between MBB is stronger than that of 3CCV, MBB-MQ starts to crystallize at a higher temperature than 3CCV-MQ. For melting point (T_m), MQ is not much different between 3CCV-MQ and MBB-MQ. No significant difference in the DSC curve of 3CCV/MBB-modified polydimethylsiloxane was found compared with α,ω -vinyl-terminated polydimethylsiloxane.

TGA was used to explore the effect of 3CCV/MBB modification on the thermal stability of dimethyl silicone rubber. We can see from Table 2 and Figure 3b that the thermal stability of 3CCV/MBB-MQ decreases to a certain extent. The MBB-MQ shows good thermal stability, and its thermal decomposition temperature is higher than 350 °C. However, the thermal decomposition temperature of 3CCV-MQ is obviously lower than that of MBB-MQ. This can be caused by the fact that the thermal stability of MBB benzene ring structure is better than that of 3CCV cyclohexane skeleton, so the 5% weight loss temperature, 10% weight loss temperature, and maximum weight loss temperature of MBB-MQ are higher than those of 3CCV-MQ. The dTG curve with temperature further proves the difference in the thermal stability of MQ, 3CCV-MQ, and MBB-MQ. As can be seen from Figure 3c, the thermal stability of 3CCV-MQ is inferior to that of MBB-MQ. In the process of heating, 3CCV/MBB liquid crystal unit with the C–C bond as the skeleton decomposes first, which affects the thermal stability of dimethyl silicone rubber. In order to ensure the severe service conditions of silicone rubber, we use liquid crystal units with high thermal stability for modification.

We used a universal tensile testing machine to study the stress–strain behavior of MQ, 3CCV-MQ, and MBB-MQ. As shown in Figure 4a and Table 3, the mechanical strength and elongation at break of 3CCV-MQ and MBB-MQ are significantly higher than that of MQ, and the mechanical adaptive platform of MBB-MQ is more obvious than that of 3CCV-MQ. In particular, the large benzene ring structure of MBB leads to stronger intermolecular forces of MBB-MQ, so

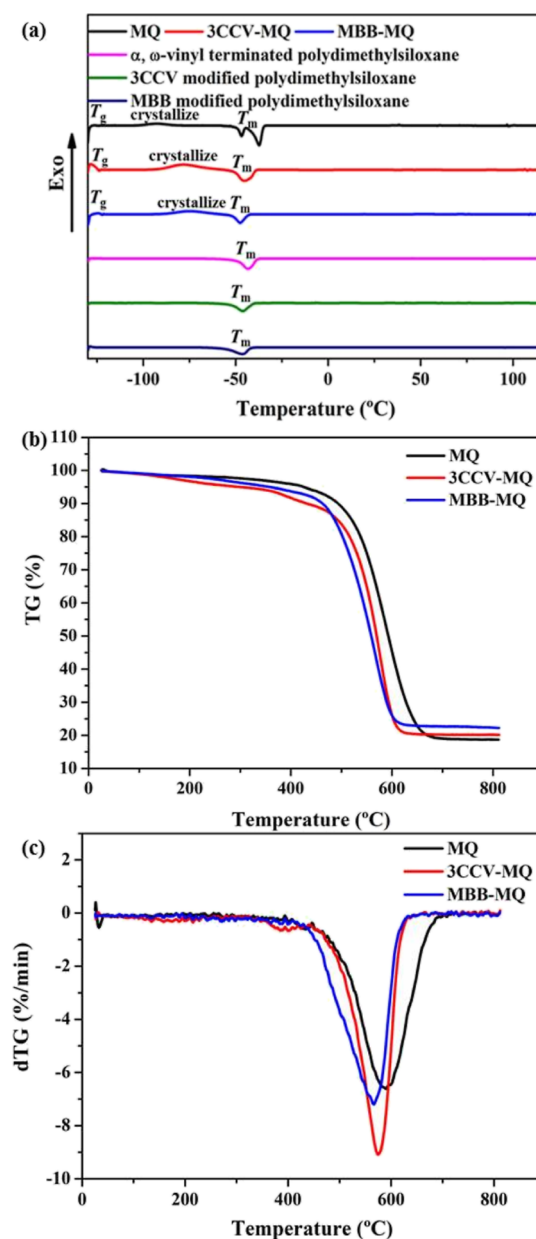


Figure 3. (a) DSC curves of MQ, 3CCV-MQ, MBB-MQ, α,ω -vinyl-terminated polydimethylsiloxane, and 3CCV- and MBB-modified polydimethylsiloxane. (b) TG and (c) dTG curves of MQ, 3CCV-MQ, and MBB-MQ.

Table 2. Summary of 5%, 10%, Maximum Weight Loss Temperature and 800 °C Residual Weight

no.	5% weight loss temperature (°C)	10% weight loss temperature (°C)	maximum weight loss temperature (°C)	800 °C residual weight (%)
MQ	425	493	704	19
3CCV-MQ	298	431	649	20
MBB-MQ	357	463	650	22

MBB-MQ exhibits higher mechanical strength and elongation at break compared with 3CCV-MQ. The mechanical strength of MBB-MQ is up to 5.83 MPa and the elongation at break is more than 10 times its own length, which are higher than those in our previous study.^{32,33} Similarly, the mechanical strength of

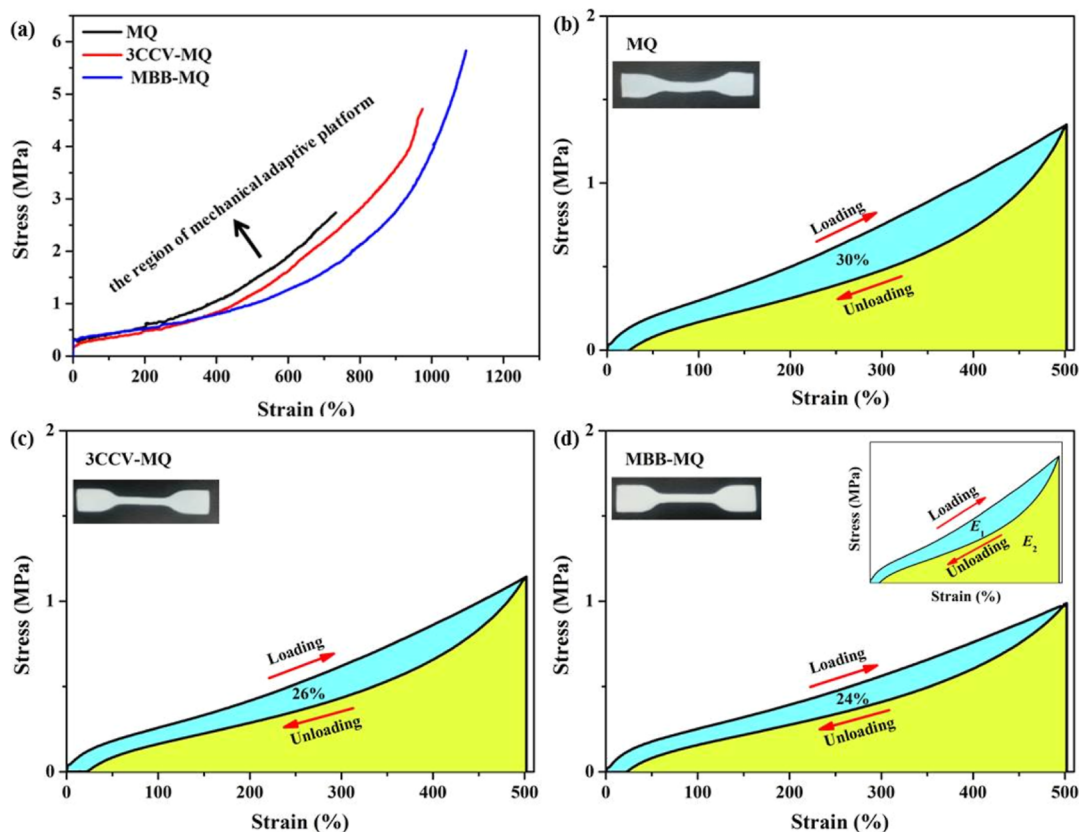


Figure 4. (a) Stress–strain curves of MQ, 3CCV-MQ, and MBB-MQ at 25 °C. The loading–unloading energy dissipation ratio of (b) MQ, (c) 3CCV-MQ, and (d) MBB-MQ at a maximum strain of 500%. The inset figure of Figure 2d illustrates the definition of the energy dissipation ratio.

Table 3. Summary of the Tensile Strength, Elongation at Break, and the Shore Hardness

no.	tensile strength (MPa)	elongation at break (%)	shore hardness (HA)
MQ	2.74 ± 0.05	733 ± 18	14
3CCV-MQ	4.71 ± 0.1	974 ± 22	15
MBB-MQ	5.83 ± 0.15	1096 ± 30	16

3CCV-MQ is also up to 4.71 MPa, and the elongation at break is more than 10 times its own length. The reason is as follows: in order to ensure the complete graft of 3CCV/MBB, thiol groups are excessive in the preparation of 3CCV/MBB-modified polydimethylsiloxane, and in the process of further click reaction, excessive thiol groups react with the terminal vinyl group of 3CCV/MBB-modified polydimethylsiloxane to achieve the effect of chain extension, which significantly improves the mechanical strength and elongation at break of 3CCV/MBB-MQ compared with MQ. It also provides a novel method for us to further improve the mechanical properties of silicone rubber. In addition, we also measured the loading–unloading energy dissipation ratio of MQ, 3CCV-MQ, and MBB-MQ when the strain is in the mechanical adaptive region (500%). The energy dissipation ratio, $R = E_1/(E_1 + E_2)$, relates the energy dissipated during the cycle to the energy absorbed by the elastomers during loading. With the enhancement of intermolecular force, the energy dissipation ratio of MQ, 3CCV-MQ, and MBB-MQ gradually decreases from 30 to 24% (Figure 4b–d). When the strain is 1000%, the energy dissipation ratio of MBB-MQ is up to 38%, which is much higher than that of 24% when the strain is 500% (Figure S2).

The cyclic loading–unloading stress–strain curves prove that the mechanical properties of the elastomers prepared by us are reliable and stable (Figure S3). When tension is applied to 3CCV/MBB-MQ, the intermolecular force between 3CCV/MBB-MQ can still dissipate energy to achieve mechanical adaptive function. In the large deformation region, the increase of stress under continuous strain is obviously suppressed and a stress plateau region appears in the stress–strain curve. The mechanical adaptive platform of 3CCV-MQ is not as obvious as MBB-MQ, but it is better than MQ. Therefore, we believe that the liquid crystal-modified dimethyl silicone rubber mechanical adaptive function is expected to be used in industrial applications as a soft connection system.

We investigate the viscoelasticity of MQ, 3CCV-MQ, and MBB-MQ by DMA. According to the decreasing trend of storage modulus and loss modulus, we can deduce that the T_g of MQ, 3CCV-MQ, and MBB-MQ is near -120 °C (Figure 5a,b). The storage modulus of MQ shows a sudden rise and then decline trend at -90 °C, which is caused by the crystallization of pure dimethyl silicone rubber. No such trend is observed in 3CCV-MQ and MBB-MQ, which further proves that the intermolecular force of 3CCV/MBB affects the crystallization of pure polydimethylsiloxane. The variation of storage modulus with the temperature at -40 °C corresponds to T_m on DSC. The storage modulus curves of 3CCV-MQ and MBB-MQ are almost coincident from -70 to 50 °C, but there are significant differences between T_g and -70 °C. Combined with DSC curves, we think that the difference is caused by the different intermolecular forces between 3CCV-MQ and MBB-MQ (Figure 5a). Figure 5b,c shows loss modulus and loss factors curves of MQ, 3CCV-MQ, and MBB-MQ changing

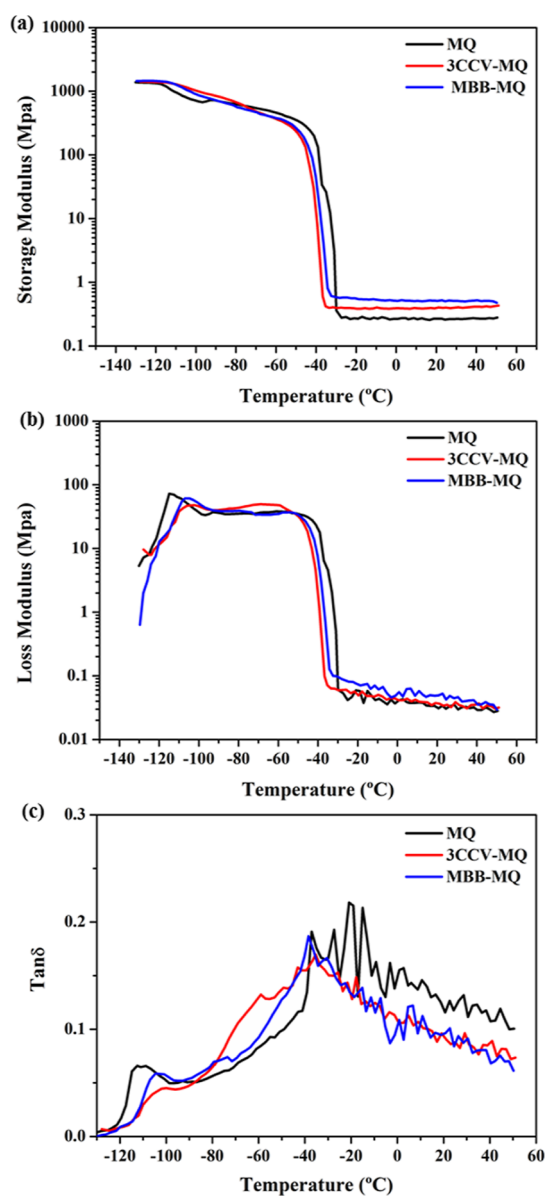


Figure 5. (a) Storage modulus curves of MQ, 3CCV-MQ, and MBB-MQ changing with temperature (b) loss modulus curves of MQ, 3CCV-MQ, and MBB-MQ changing with temperature (c) loss factor curves of MQ, 3CCV-MQ, and MBB-MQ changing with temperature.

with temperature, respectively. As shown in Figure 5c, the loss factor of 3CCV/MBB-MQ above T_m is smaller than MQ, which indicates that 3CCV/MBB modification can reduce the damping performance of silicone rubber. The loss factor of 3CCV-MQ and MBB-MQ becomes smaller and smaller as the temperature rises from T_m to 50 °C. Moreover, the two curves basically coincide, and there is no significant difference in damping performance, which is also consistent with previous results.

CONCLUSIONS

In conclusion, we developed a novel strategy to prepare a liquid crystal-modified polydimethylsiloxane rubber with mechanical adaptability. The results show that the intermolecular force between 3CCV/MBB-MQ can effectively dissipate energy to achieve mechanical adaptive function, and the mechanical adaptive platform of MBB-MQ is more obvious

than 3CCV-MQ. With the enhancement of the intermolecular force, the energy dissipation ratio of MQ, 3CCV-MQ, and MBB-MQ gradually decreases from 30 to 24%. Excessive thiol groups of 3CCV/MBB-modified polydimethylsiloxane react with its terminal vinyl group to achieve the chain extension, leading to obviously improved mechanical properties of 3CCV/MBB-MQ compared with MQ. This research pioneered a new method to improve the mechanical strength of silicone rubber and provided guidance for the design and preparation of new mechanical adaptive materials.

ASSOCIATED CONTENT

Supporting Information

The Supporting Information is available free of charge at <https://pubs.acs.org/doi/10.1021/acsomega.2c04560>.

Materials; Characterization of polydimethylsiloxane; Synthesis of 3CCV-modified polydimethylsiloxane and MBB-modified polydimethylsiloxane; The preparation of MQ and 3CCV/MBB-MQ; The composition of 3CCV and MBB-modified polydimethylsiloxane; The composition of MQ, 3CCV-MQ, and MBB-MQ; Proportion of crosslinking chains, dangling chains, free chains and the cross-linked density in MQ, 3CCV-MQ, and MBB-MQ; ^1H NMR spectra of hydroxyl-terminated mercaptopropyl silicone oil prepolymer; Loading–unloading energy dissipation ratio of MBB-MQ at a maximum strain of 1000% and Cyclic loading–unloading stress–strain curves of MQ, 3CCV-MQ, MBB-MQ at a maximum strain of 500% and MBB-MQ at a maximum strain of 1000% (PDF)

AUTHOR INFORMATION

Corresponding Authors

Hua Wang – School of Materials Science and Engineering, Shandong University, Jinan 250061, China; Email: hwang@sdu.edu.cn

Chuanjian Zhou – School of Materials Science and Engineering, Shandong University, Jinan 250061, China; orcid.org/0000-0003-3567-2993; Email: Zhouchuanjian@sdu.edu.cn

Author

Zhe Liu – School of Materials Science and Engineering, Shandong University, Jinan 250061, China

Complete contact information is available at: <https://pubs.acs.org/10.1021/acsomega.2c04560>

Notes

The authors declare no competing financial interest.

ACKNOWLEDGMENTS

The authors are thankful for the financial support from the National Natural Science Foundation of China (U2030203) and the Joint Fund of Natural Science Foundation of Shandong Province (ZR2021LFG005).

REFERENCES

- Qiu, Y.; Zhang, E.; Plamthottam, R.; Pei, Q. B. Dielectric elastomer artificial muscle: materials innovations and device explorations. *Acc. Chem. Res.* **2019**, *52*, 316–325.
- Ling, Y.; Pang, W. B.; Liu, J. X.; Page, M.; Xu, Y. D.; Zhao, G. G.; Stalla, D.; Xie, J. W.; Zhang, Y. H.; Yan, Z. Bioinspired elastomer

composites with programmed mechanical and electrical anisotropies. *Nat. Commun.* **2022**, *13*, 524.

(3) Tu, Z. K.; Liu, W. F.; Wang, J.; Qiu, X. Q.; Huang, J. H.; Li, J. X.; Lou, H. M. Biomimetic high performance artificial muscle built on sacrificial coordination network and mechanical training process. *Nat. Commun.* **2021**, *12*, 2916.

(4) Li, H. J.; Zheng, H.; Tan, Y. J.; Tor, S. B.; Zhou, K. Development of an ultrastretchable double-network hydrogel for flexible strain sensors. *ACS Appl. Mater. Interfaces* **2021**, *13*, 12814–12823.

(5) Huang, J.; Xu, Y. C.; Qi, S. H.; Zhou, J. J.; Shi, W.; Zhao, T. Y.; Liu, M. J. Ultrahigh energy-dissipation elastomers by precisely tailoring the relaxation of confined polymer fluids. *Nat. Commun.* **2021**, *12*, 3610.

(6) Guo, J. Y.; Zehnder, A. T.; Creton, C.; Hui, C. Y. Time dependent fracture of soft materials: linear versus nonlinear viscoelasticity. *Soft Matter* **2020**, *16*, 6163–6179.

(7) Weisgraber, T. H.; Metz, T.; Spadaccini, C. M.; Duoss, E. B.; Small, W.; Lenhardt, J. M.; Maxwell, R. S.; Wilson, T. S. A mechanical reduced order model for elastomeric 3D printed architectures. *J. Mater. Res.* **2018**, *33*, 309–316.

(8) Yu, S.; Chai, H.; Xiong, Y.; Kang, M.; Geng, C.; Liu, Y.; Chen, Y.; Zhang, Y.; Zhang, Q.; Li, C.; Wei, H.; Zhao, Y.; Yu, F.; Lu, A. Studying complex evolution of hyperelastic materials under external field stimuli using artificial neural networks with spatiotemporal features in a small-scale dataset. *Adv. Mater.* **2022**, *34*, 2200908.

(9) Wang, Z.; Guo, Y.; Cai, S.; Yang, J. Three-Dimensional Printing of Liquid Crystal Elastomers and Their Applications. *ACS Appl. Mater. Interfaces* **2022**, *4*, 3153–3168.

(10) Ohzono, T.; Saed, M. O.; Terentjev, E. M. Enhanced Dynamic Adhesion in Nematic Liquid Crystal Elastomers. *Adv. Mater.* **2019**, *31*, 1902642.

(11) Traugutt, N. A.; Mistry, D.; Luo, C. Q.; Yu, K.; Ge, Q.; Yakacki, C. M. Liquid-Crystal-Elastomer-Based Dissipative Structures by Digital Light Processing 3D Printing. *Adv. Mater.* **2020**, *32*, 2000797.

(12) Ma, C.; Wu, S.; Ze, Q.; Kuang, X.; Zhang, R.; Qi, H. J.; Zhao, R. Magnetic Multimaterial Printing for Multimodal Shape Transformation with Tunable Properties and Shiftable Mechanical Behaviors. *ACS Appl. Mater. Interfaces* **2020**, *13*, 12639–12648.

(13) Liu, Z.; Bisoyi, H. K.; Huang, Y.; Wang, M.; Yang, H.; Li, Q. Thermo- and Mechanochromic Camouflage and Self-Healing in Biomimetic Soft Actuators Based on Liquid Crystal Elastomers. *Angew. Chem., Int. Ed.* **2022**, *61*, No. e202115755.

(14) Wang, M.; Song, Y.; Bisoyi, H. K.; Yang, J. F.; Liu, L.; Yang, H.; Li, Q. A Liquid Crystal Elastomer-Based Unprecedented Two-Way Shape-Memory Aerogel. *Adv. Sci.* **2021**, *8*, 2102674.

(15) Luo, C.; Chung, C.; Traugutt, N. A.; Yakacki, C. M.; Long, K. N.; Yu, K. 3D Printing of Liquid Crystal Elastomer Foams for Enhanced Energy Dissipation Under Mechanical Insult. *ACS Appl. Mater. Interfaces* **2020**, *13*, 12698–12708.

(16) Merkel, D. R.; Shaha, R. K.; Yakacki, C. M.; Frick, C. P. Mechanical energy dissipation in polydomain nematic liquid crystal elastomers in response to oscillating loading. *Polymer* **2019**, *166*, 148–154.

(17) Rešetič, A.; Milavec, J.; Zupančič, B.; Domenici, V.; Zalar, B. Polymer-dispersed liquid crystal elastomers. *Nat. Commun.* **2016**, *7*, 13140.

(18) Ware, T. H.; Biggins, J. S.; Shick, A. F.; Warner, M.; White, T. J. Localized soft elasticity in liquid crystal elastomers. *Nat. Commun.* **2016**, *7*, 10781.

(19) Annapooranan, R.; Wang, Y.; Cai, S. Q. Highly Durable and Tough Liquid Crystal Elastomers. *ACS Appl. Mater. Interfaces* **2022**, *14*, 2006–2014.

(20) Donovan, B. R.; Fowler, H. E.; Matavulj, V. M.; White, T. J. Mechanotropic Elastomers. *Angew. Chem., Int. Ed.* **2019**, *58*, 13744–13748.

(21) Yang, H.; Liu, J.-J.; Wang, Z.-F.; Guo, L.-X.; Keller, P.; Lin, B.-P.; Sun, Y.; Zhang, X.-Q. Near-infrared-responsive gold nanorod/liquid crystalline elastomer composites prepared by sequential thiol-click chemistry. *Chem. Commun.* **2015**, *51*, 12126–12129.

(22) Yang, H.; Liu, M.-X.; Yao, Y.-W.; Tao, P.-Y.; Lin, B.-P.; Keller, P.; Zhang, X.-Q.; Sun, Y.; Guo, L.-X. Polysiloxane-Based Liquid Crystalline Polymers and Elastomers Prepared by Thiol–Ene Chemistry. *Macromolecules* **2013**, *46*, 3406–3416.

(23) Wang, L.; Liu, W.; Guo, L.-X.; Lin, B.-P.; Zhang, X.-Q.; Sun, Y.; Yang, H. A room-temperature two-stage thiol–ene photoaddition approach towards monodomain liquid crystalline elastomers. *Polym. Chem.* **2017**, *8*, 1364–1370.

(24) Wang, Z. J.; Tian, H. M.; He, Q. G.; Cai, S. Q. Reprogrammable, Reprocessible, and Self-Healable Liquid Crystal Elastomer with Exchangeable Disulfide Bonds. *ACS Appl. Mater. Interfaces* **2017**, *9*, 33119–33128.

(25) Boothby, J. M.; Ware, T. H. Dual-responsive, shape-switching bilayers enabled by liquid crystal elastomers. *Soft Matter* **2017**, *13*, 4349–4356.

(26) Shaha, R. K.; Torbati, A. H.; Frick, C. P. Body-temperature-shape-shifting liquid crystal elastomers. *J. Appl. Polym. Sci.* **2021**, *138*, 50136.

(27) Thomsen, D. L.; Keller, P.; Naciri, J.; Pink, R.; Jeon, H.; Shenoy, D.; Ratna, B. R. Liquid Crystal Elastomers with Mechanical Properties of a Muscle. *Macromolecules* **2001**, *34*, 5868–5875.

(28) Tian, H. M.; Wang, Z. J.; Chen, Y. L.; Shao, J. Y.; Gao, T.; Cai, S. Q. Polydopamine-Coated Main-Chain Liquid Crystal Elastomer as Optically Driven Artificial Muscle. *ACS Appl. Mater. Interfaces* **2018**, *10*, 8307–8316.

(29) Li, Y. F. S.; Zang, C. G.; Zhang, Y. L. Effect of the structure of hydrogen-containing silicone oil on the properties of silicone rubber. *Mater. Chem. Phys.* **2020**, *248*, 122734.

(30) Wang, Z.; Li, W.; Chen, L.; Zhan, Z.; Duan, H. 3D Printable Silicone Rubber for Long-Lasting and Weather-Resistant Wearable Devices. *ACS Appl. Polym. Mater.* **2022**, *4*, 2384–2392.

(31) Wang, G. F.; Li, A. L.; Zhao, W.; Xu, Z. H.; Ma, Y. W.; Zhang, F. Y.; Zhang, Y. B.; Zhou, J.; He, Q. A Review on Fabrication Methods and Research Progress of Superhydrophobic Silicone Rubber Materials. *Adv. Mater. Interfac.* **2021**, *8*, 2001460.

(32) Liu, Z.; Xiong, Y. Q.; Hao, J. H.; Zhang, H.; Cheng, X.; Wang, H.; Chen, W.; Zhou, C. J. Liquid Crystal-Based Organosilicone Elastomers with Supreme Mechanical Adaptability. *Polymers* **2022**, *14*, 789.

(33) Liu, Z.; Wang, H.; Zhou, C. J. The Effect of Phenyl Content on the Liquid Crystal-Based Organosilicone Elastomers with Mechanical Adaptability. *Polymers* **2022**, *14*, 903.

(34) Park, J. J.; Lee, J. Y.; Hong, Y. G. Effects of vinylsilane-modified nanosilica particles on electrical and mechanical properties of silicone rubber nanocomposites. *Polymer* **2020**, *197*, 122493.

(35) Wang, J. J.; Feng, L. J.; Lei, A. L.; Yan, A. J.; Wang, X. J. Thermal stability and mechanical properties of room temperature vulcanized silicone rubbers. *J. Appl. Polym. Sci.* **2012**, *125*, 505–511.

(36) Hao, D.; Li, D. X.; Liao, Y. H. Hyperelasticity, dynamic mechanical property, and rheology of addition-type silicone rubber (VPDMS cured by PMHS). *J. Appl. Polym. Sci.* **2015**, *132*, 42036.

(37) Zhou, W. Y.; Qi, S. H.; Tu, C. C.; Zhao, H. Z. Novel heat-conductive composite silicone rubber. *J. Appl. Polym. Sci.* **2007**, *104*, 2478–2483.

(38) Lee, S. B.; Kim, Y. J.; Ko, U.; Min, C. M.; Ahn, M. K.; Chung, S. J.; Moon, I. S.; Lee, J. S. Sulfonated poly(arylene ether) membranes containing perfluorocyclobutyl and ethynyl groups: Increased mechanical strength through chain extension and crosslinking. *J. Membr. Sci.* **2014**, *456*, 49–56.

(39) Baimark, Y.; Pasee, S.; Rungseesantivanon, W.; Prakymoram, N. Flexible and high heat-resistant stereocomplex PLLA-PEG-PLLA/PDLA blends prepared by melt process: effect of chain extension. *J. Polym. Res.* **2019**, *26*, 218.

(40) Dvornic, P. R.; Lenz, R. W. Exactly alternating silarylene-siloxane polymers. 9. Relationships between polymer structure and glass transition temperature. *Macromolecules* **2002**, *25*, 3769–3778.

(41) Tang, Y.; Tsiang, R. Rheological, extractive and thermal studies of the room temperature vulcanized polydimethylsiloxane. *Polymer* **1999**, *40*, 6135–6146.